



저작자표시-비영리-변경금지 2.0 대한민국

이용자는 아래의 조건을 따르는 경우에 한하여 자유롭게

- 이 저작물을 복제, 배포, 전송, 전시, 공연 및 방송할 수 있습니다.

다음과 같은 조건을 따라야 합니다:



저작자표시. 귀하는 원저작자를 표시하여야 합니다.



비영리. 귀하는 이 저작물을 영리 목적으로 이용할 수 없습니다.



변경금지. 귀하는 이 저작물을 개작, 변형 또는 가공할 수 없습니다.

- 귀하는, 이 저작물의 재이용이나 배포의 경우, 이 저작물에 적용된 이용허락조건을 명확하게 나타내어야 합니다.
- 저작권자로부터 별도의 허가를 받으면 이러한 조건들은 적용되지 않습니다.

저작권법에 따른 이용자의 권리는 위의 내용에 의하여 영향을 받지 않습니다.

이것은 [이용허락규약\(Legal Code\)](#)을 이해하기 쉽게 요약한 것입니다.

[Disclaimer](#)

**M. S. Thesis**

**Opportunistic CSI Feedback  
in Multi-user MIMO Environments**

다중 사용자 다중 안테나 환경에서  
기회적 채널정보 궤환 기법 연구

**by**

**Jeong-Soo Park**

**August 2012**

**School of Electrical Engineering and Computer Science**

**College of Engineering**

**Seoul National University**

# Abstract

The application of multi-input multi-out (MIMO) techniques to wireless systems has been receiving great attention as one of major potentials for the improvement of transmission capacity. The base station can employ MIMO techniques to improve the user signal-to-noise power ratio (SNR) or to simultaneously transmit multiple transmit beams to multiple users. The MIMO technique may need the use of channel state information (CSI) for better operation, including channel quality information (CQI) and channel direction information (CDI). The CSI is often reported from mobile stations in a quantized format, which may cause serious performance degradation.

The CSI can opportunistically be reported from users, which can reduce the feedback signaling overhead while achieving multi-user diversity gain. Most of opportunistic feedback schemes use the CQI as a primary reference for the CSI. However, the use of quantized CDI for MIMO transmission may cause inter-beam interference among multiple transmit beams as well as beamforming gain reduction. As a consequence, it may be desirable to consider the CDI as well as the CQI.

In this thesis, we consider the CQI and the CDI for the opportunistic CSI feedback.

We analyze the effect of CSI quantization error on the beamforming performance in multi-user MIMO environments. Then, we propose a novel scheme for opportunistic feedback and user scheduling in single-user beamforming and multi-user spatial multiplexing environments. Simulation results show that the proposed scheme can improve the spectral efficiency using a small amount of CSI feedback signaling overhead.

**Keywords:** opportunistic feedback, codebook, channel direction information, beamforming, quantization error

**Student number:** 2010-23266

# Contents

Abstract .....	i
Contents .....	iii
List of Figures .....	v
List of Tables.....	vi
1. Introduction.....	1
2. System model.....	5
2.1. Multi-user MIMO system.....	5
2.2. Channel.....	8
2.2.1. Channel quality information.....	8
2.2.2. Channel direction information.....	9
3. Motivation.....	12
3.1. Performance of multi-user MIMO schemes .....	12
3.2. Previous opportunistic CSI feedback schemes .....	21
3.2.1. Absolute SNR-based single user scheduling (ASS).....	21
3.2.2. Normalized SNR-based scheduling (NSS).....	21
3.2.3. Advanced normalized SNR-based scheduling (A-NSS) .....	22

3.2.4.    Limitation in the opportunistic CSI feedback schemes .....	23
4. Proposed opportunistic CSI feedback.....	24
4.1. Single-user beamforming.....	24
4.2. Multi-user spatial multiplexing.....	29
4.3. Performance evaluation .....	32
5. Conclusions.....	41
References .....	42
초 록.....	44

# List of Figures

Fig. 2. 1. A multi-user MISO cellular operation environment .....	6
Fig. 2. 2. The pdf of channel power and channel direction.....	11
Fig. 3. 1. Visual representation of $\hat{\mathbf{h}}_k$ , $\mathbf{w}_k$ , $\mathbf{g}_k^*$ , and $\mathbf{g}_k$ .....	16
Fig. 3. 2. Spectral efficiency of zero-forcing beamforming ( $N_T = 4$ ) .....	20
Fig. 4. 1. The pdf and cdf of $\mu$ when $N_T = 4$ .....	28
Fig. 4. 2. Performance of the proposed scheme with single-user beamforming. .	36
Fig. 4. 3. Performance of the proposed scheme with multi-user spatial multiplexing.....	40

# List of Tables

Table. 4. 1. Simulation parameter.....	33
--	----



# 1. Introduction

The use of multi-input multi-output (MIMO) antenna techniques has received great attention for its potential to increase the transmission capacity of wireless cellular systems [1]. It is known that the spectral efficiency can be increased linearly proportional to the number of transmit antennas [2]. Multiple antennas can be used to provide transmit diversity to a serving user with single-user beamforming (SUBF). They can also be used to generate multiple beams in parallel, referred to multi-user spatial multiplexing (MUSM). The MUSM is employed in high signal-to-interference plus noise power ratio (SINR) environments, whereas the SUBF is employed in low-SINR environments [3].

When a base station (BS) services multiple users, it can improve the spectral efficiency by exploiting multi-user diversity (MUD). It is shown that as the number of users increases, the MUD gain increases [4]. The MUD gain has well been studied in single-input single-output (SISO) environments [4] and spatially correlated MIMO environments [5]. However, the theoretical performance may not be achievable in practical environments due to impairments such as signaling overhead for the feedback of user information. Each user reports channel state information (CSI),

including channel direction information (CDI) and channel quality information (CQI), to the serving base station (BS) for closed-loop MIMO operation. The CSI is represented using a small number of bits, yielding unavoidable quantization error which may severely degrade the MIMO performance [6]. It may be desirable to represent the CSI to reduce the quantization error without increasing the bit size.

Recent works consider opportunistic feedback of CSI, where users in good channel condition can only report their CSI to the BS, significantly reducing the amount of CSI feedback. A simple scheme allows users to report their CQI only when their signal-to-noise power ratio (SNR) is higher than a certain level, referred to the absolute SNR based scheduling (ASS) [7]. The ASS can considerably reduce the feedback signaling overhead while achieving the MUD gain. However, it may cause scheduling unfairness in heterogeneous channel environments, where users experience different average SNR. This scheduling unfairness problem can somewhat be alleviated with the use of normalized SNR for the scheduling (referred to the NSS) [8]. The NSS scheme schedules users based on instantaneous SNR normalized in terms of its average SNR. However, the channel correlation can affect the variance of MIMO channel SNR, which may still involve scheduling unfairness. This scheduling fairness problem can significantly be alleviated with the use of instantaneous SNR normalized in terms of its average and variance [9], referred to the advanced normalized SNR based scheduling (A-NSS).

The BS needs the CDI as well as the CQI for better MIMO operation, where the CDI is often represented using a codebook in practice. When the CDI is represented using a codebook with a small bit size, it may trigger channel mismatch problem that may cause beamforming gain reduction in the SUBF operation and inter-beam interference in the MUSM operation. It may be desirable to additionally consider the effect of CDI for the opportunistic feedback.

In this thesis, we design an opportunistic feedback scheme in multi-user MIMO environments, considering the effect of CQI and CDI as well. We first analyze the effect of the CDI quantization error on the SUBF and the MUSM. The CDI quantization error may yield the channel mismatch problem, reducing the beamforming gain of the SUBF operation. This problem can be alleviated by allowing users with higher expected channel gain to report their CSI to the BS. By exploiting the MUD gain with reduced feedback signaling overhead, we can improve the performance of SUBF operation. On the other hand, the CDI quantization error may yield inter-beam interference in the MUSM operation. This problem can be alleviated by allowing users with smaller CDI quantization error to report their CSI to the BS. Thus, we can achieve further performance improvement over the scheme that uses the CSI of all users, while effectively eliminating the inter-beam interference.

The rest of the thesis is organized as follows. Chapter 2 describes the system and channel model in consideration. Chapter 3 reviews previous works on opportunistic

CSI feedback schemes and introduces motivation for the proposed opportunistic feedback scheme with capacity analysis of the SUBF and the MUSM. Chapter 4 describes the proposed opportunistic feedback and user scheduling scheme, and verifies it by computer simulation. Chapter 5 summarizes conclusions.

## 2. System model

### 2.1. Multi-user MIMO system

Fig. 2.1. illustrates the down-link of a multi-user cellular system, where the BS is equipped with  $N_T$  transmit antennas and  $K$  users are equipped with a single receive antenna (i.e., multi-input single-output (MISO) environments). We assume that the BS simultaneously serves  $M (\leq N_T)$  users using the same time and frequency resource by means of transmit precoding. Then, the received signal of user  $k$  can be represented as

$$y_k = \sqrt{\alpha_k} \mathbf{h}_k \sum_{m=1}^M \mathbf{w}_m^H x_m + n_k \quad (2-1)$$

where  $\alpha_k$  denotes large-scale fading between the BS and user  $k$ ,  $\mathbf{h}_k (= [h_k^{(1)} \ h_k^{(2)} \ \dots \ h_k^{(N_T)}])$  denotes the  $(1 \times N_T)$  small-scale fading vector between the BS and user  $k$ ,  $\mathbf{w}_m$  denotes the  $(1 \times N_T)$  beam weight vector for serving user  $m$ , the superscript  $H$  denotes the conjugate transpose operator,  $x_m$  denotes the data transmitted to user  $m$  with transmit power  $P/M (= E\{|x_m|^2\})$ , and  $n_k$  denotes zero-mean additive white Gaussian noise (AWGN) with variance  $\sigma_n^2$ .

For closed-loop beamforming, each user reports its CDI to the serving BS. Assuming that users report their CDI by means of codebook quantization with  $B$ -bit [9], it can be represented as

$$\begin{aligned}\hat{\mathbf{h}}_k &= \arg \max_{\mathbf{c}_i \in \mathcal{C}} \left( \left| \mathbf{c}_i \cdot \tilde{\mathbf{h}}_k \right|^2 \right) \\ &= \arg \max_{\mathbf{c}_i \in \mathcal{C}} \left( \left| \mathbf{c}_i \tilde{\mathbf{h}}_k^H \right|^2 \right)\end{aligned}\quad (2-2)$$

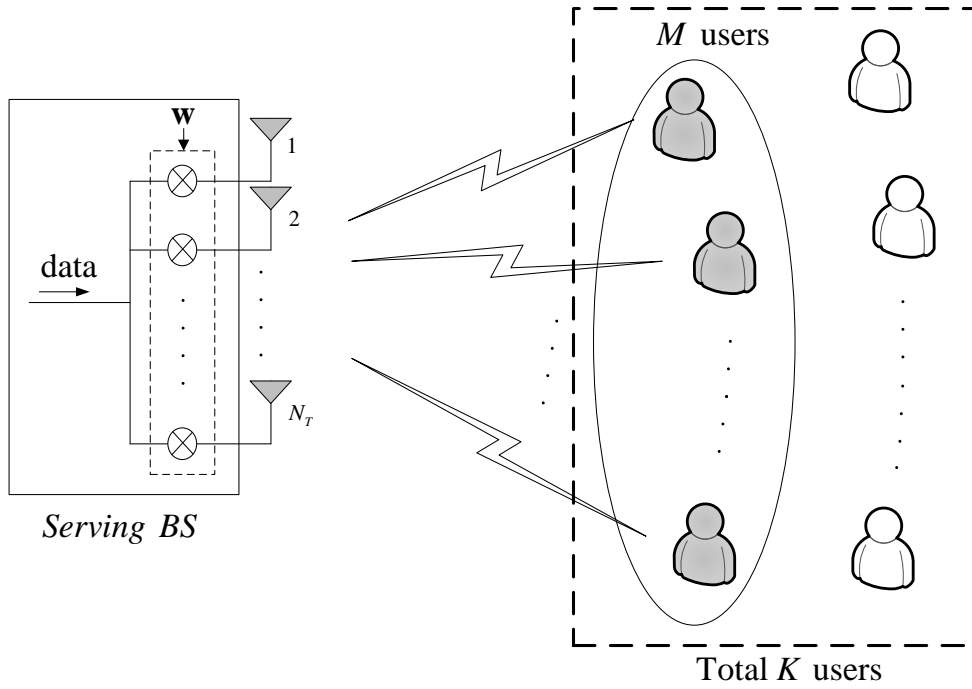


**Fig. 2. 1. A multi-user MISO cellular operation environment**

where  $\tilde{\mathbf{h}}_k (\triangleq \mathbf{h}_k / \|\mathbf{h}_k\|)$  denotes the normalized channel,  $C (= \{\mathbf{c}_1, \mathbf{c}_2, \dots, \mathbf{c}_{2^B}\})$  denotes a set of code-words in the  $B$ -bit codebook, and  $\mathbf{c}_i$  denotes the  $i$ -th codeword in the codebook.

When the BS employs coherent beamforming (CBF) (i.e.,  $M = 1$ ) for the transmission of user signal, the beam weight vector for user  $k$  can be represented as

$$\mathbf{w}_k = \hat{\mathbf{h}}_k^H. \quad (2-3)$$

On the other hand, the BS can generate multiple beams to simultaneously serve multiple users using the same time and frequency resource. When the BS serves  $M$  users using zero-forcing beamforming (ZFBF), the beam weight vector  $\mathbf{w}_k$  for user  $k$  satisfies the following condition [10]

$$\mathbf{w}_k = \arg \max_{\mathbf{w} \in \Omega_k} \left( \left| \hat{\mathbf{h}}_k \cdot \mathbf{w} \right|^2 \right) \quad (2-4)$$

where the beam weight set  $\Omega_k$  is defined by

$$\Omega_k \triangleq \left\{ \mathbf{w} \mid \left| \hat{\mathbf{h}}_m \cdot \mathbf{w} \right|^2 = 0, \forall m \in \Psi, m \neq k \right\}. \quad (2-5)$$

Here  $\Psi$  denotes a set of spatially multiplexed users.

## 2.2. Channel

### 2.2.1. Channel quality information

Let  $\mathbf{h}_k (= [h_k^{(1)} \ h_k^{(2)} \ \dots \ h_k^{(N_T)}])$  be a random vector whose elements are independent and identically distributed (i.i.d.) zero-mean complex Gaussian random variables with unit variance. The probability density function (pdf) of  $X_p^{(i)} \triangleq |h_k^{(i)}|^2$  for  $1 \leq i \leq N_T$  can be represented as [11]

$$f_{X_p^{(i)}}(x) = e^{-x}. \quad (2-6)$$

That is,  $X_p^{(i)}$  is an exponentially distributed random variable with unit variance. The corresponding characteristic function can be represented as

$$\Phi_{X_p^{(i)}}(\omega) = \frac{1}{1 - i\omega}. \quad (2-7)$$

The power of the channel vector  $\|\mathbf{h}_k\|^2 = \sum_{i=1}^{N_T} |h_k^{(i)}|^2$  is a sum of the power of each element. The characteristic function of  $X_p \triangleq \|\mathbf{h}_k\|^2$  can be represented as [11]

$$\Phi_{X_p}(\omega) = \frac{1}{(1 - i\omega)^{N_T}}. \quad (2-8)$$

It can be shown that  $X_p$  has Erlang distribution with the pdf represented as



$$f_{X_p}(x) = \begin{cases} \frac{x^{N_T-1} e^{-x}}{\Gamma(N_T)}, & x \geq 0 \\ 0, & x < 0 \end{cases} \quad (2-9)$$

where  $\Gamma(\bullet)$  denotes Gamma function. Thus, it can be shown that the mean of  $X_p$  is

$$\begin{aligned} E\{X_p\} &= \int_{-\infty}^{\infty} x f_{X_p}(x) dx \\ &= N_T. \end{aligned} \quad (2-10)$$

### 2.2.2. Channel direction information

Assuming that the channel elements  $\{h_k^{(1)}, h_k^{(2)}, \dots, h_k^{(N_T)}\}$  are i.i.d.,  $\tilde{\mathbf{h}}_k$  can be considered as a unit random vector whose direction is uniformly distributed in an  $N_T$ -dimensional complex space. Letting  $\mathbf{v}$  be a unit vector in an  $N_T$ -dimensional complex space, it can be shown from [6] that  $X_D = |\tilde{\mathbf{h}}_k \cdot \mathbf{v}|^2$  has Beta distribution with  $\alpha = 1$  and  $\beta = N_T - 1$ , whose pdf is represented as,

$$f_X(x; \alpha, \beta) = \begin{cases} \frac{x^{\alpha-1} (1-x)^{\beta-1}}{\int_0^1 u^{\alpha-1} (1-u)^{\beta-1} du}, & 0 \leq x \leq 1 \\ 0, & \text{otherwise} \end{cases}. \quad (2-11)$$

Thus, the pdf of  $X_D$  can be represented as

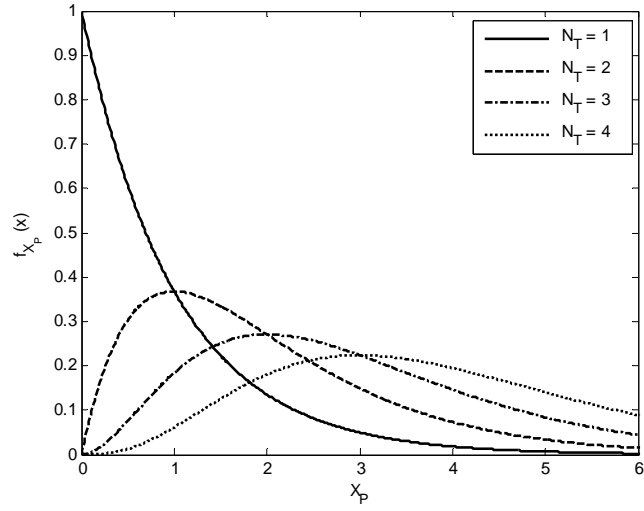
$$f_{X_D}(x) = \begin{cases} (N_T - 1)(1-x)^{N_T-2}, & 0 \leq x \leq 1 \\ 0, & \text{otherwise} \end{cases}. \quad (2-12)$$

Note that  $X_D$  can be treated as  $\cos^2 \theta$ , where  $\theta$  denotes the angle between  $\tilde{\mathbf{h}}_k$

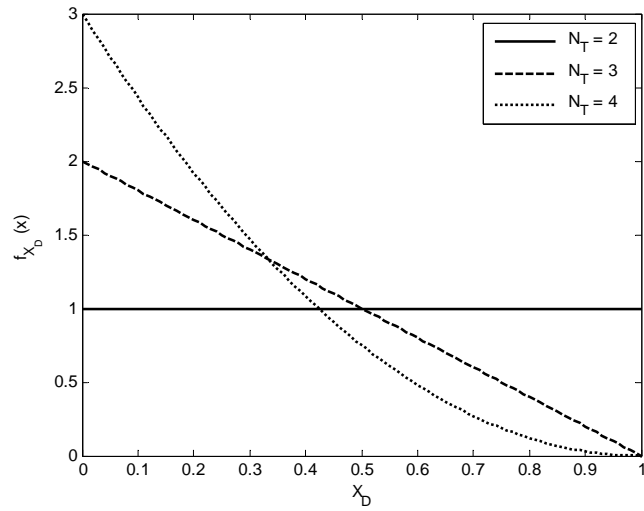
and  $\mathbf{v}$ . It can be seen that

$$\begin{aligned} E\{X_D\} &= \int_{-\infty}^{\infty} x f_{X_D}(x) dx \\ &= \frac{1}{N_T}. \end{aligned} \tag{2-13}$$

Fig. 2.2. (a) and (b) respectively depict the pdf of channel power  $X_p$  and channel direction  $X_D$  according to the number of transmit antennas.



(a) The pdf of channel power (Erlang distribution)



(b) The pdf of channel direction (Beta distribution)

**Fig. 2. 2. The pdf of channel power and channel direction.**

## 3. Motivation

### 3.1. Performance of multi-user MIMO schemes

The post SINR of user  $k$  associated with (2-1) can be represented as

$$\begin{aligned} \gamma_k &= \frac{|\mathbf{h}_k \cdot \mathbf{w}_k|^2 \frac{\alpha P}{M}}{\sum_{\substack{m=1 \\ m \neq k}}^M |\mathbf{h}_k \cdot \mathbf{w}_m|^2 \frac{\alpha P}{M} + \sigma_n^2} \\ &= \frac{\|\mathbf{h}_k\|^2 \left| \tilde{\mathbf{h}}_k \cdot \mathbf{w}_k \right|^2 \frac{\alpha P}{M}}{\|\mathbf{h}_k\|^2 \sum_{\substack{m=1 \\ m \neq k}}^M \left| \tilde{\mathbf{h}}_k \cdot \mathbf{w}_m \right|^2 \frac{\alpha P}{M} + \sigma_n^2}. \end{aligned} \quad (3-1)$$

Here, the channel direction vector  $\tilde{\mathbf{h}}_k$  can be represented in terms of the quantized channel vector  $\hat{\mathbf{h}}_k$  as [6]

$$\tilde{\mathbf{h}}_k = (\cos \theta) \hat{\mathbf{h}}_k + (\sin \theta) \mathbf{g}_k \quad (3-2)$$

where  $\mathbf{g}_k$  denotes a unit norm vector isotropically distributed in the null space of

$\hat{\mathbf{h}}_k$  and  $\cos \theta = \tilde{\mathbf{h}}_k \cdot \hat{\mathbf{h}}_k$ . Thus, (3-1) can be rewritten as

$$\begin{aligned}
\gamma_k &= \frac{\|\mathbf{h}_k\|^2 \left| (\cos \theta \hat{\mathbf{h}}_k + \sin \theta \mathbf{g}_k) \cdot \mathbf{w}_k \right|^2 \frac{\alpha P}{M}}{\|\mathbf{h}_k\|^2 \sum_{\substack{m=1 \\ m \neq k}}^M \left| (\cos \theta \hat{\mathbf{h}}_k + \sin \theta \mathbf{g}_k) \cdot \mathbf{w}_m \right|^2 \frac{\alpha P}{M} + \sigma_n^2} \\
&= \frac{\|\mathbf{h}_k\|^2 \left[ \cos^2 \theta \left| \hat{\mathbf{h}}_k \cdot \mathbf{w}_k \right|^2 + \sin^2 \theta \left| \mathbf{g}_k \cdot \mathbf{w}_k \right|^2 + 2 \cos \theta \sin \theta \left\{ \left( \hat{\mathbf{h}}_k \cdot \mathbf{w}_k \right) \times \left( \mathbf{g}_k \cdot \mathbf{w}_k \right) \right\} \right] \frac{\alpha P}{M}}{\|\mathbf{h}_k\|^2 \sin^2 \theta \sum_{\substack{m=1 \\ m \neq k}}^M \left| \mathbf{g}_k \cdot \mathbf{w}_m \right|^2 \frac{\alpha P}{M} + \sigma_n^2}. \tag{3-3}
\end{aligned}$$

Since the channel power and the channel direction are independent of each other, the average post SINR can be approximated using the first order Taylor expansion as

$$\begin{aligned}
\bar{\gamma}_k &\approx \frac{E \left\{ \|\mathbf{h}_k\|^2 \right\} \left[ E \left\{ \cos^2 \theta \right\} E \left\{ \left| \hat{\mathbf{h}}_k \cdot \mathbf{w}_k \right|^2 \right\} + E \left\{ \sin^2 \theta \right\} E \left\{ \left| \mathbf{g}_k \cdot \mathbf{w}_k \right|^2 \right\} \right] \frac{\alpha P}{M}}{E \left\{ \|\mathbf{h}_k\|^2 \right\} E \left\{ \sin^2 \theta \right\} \sum_{\substack{m=1 \\ m \neq k}}^M E \left\{ \left| \mathbf{g}_k \cdot \mathbf{w}_m \right|^2 \right\} \frac{\alpha P}{M} + \sigma_n^2} \\
&= \frac{N_T \left[ E \left\{ \cos^2 \theta \right\} E \left\{ \left| \hat{\mathbf{h}}_k \cdot \mathbf{w}_k \right|^2 \right\} + E \left\{ \sin^2 \theta \right\} E \left\{ \left| \mathbf{g}_k \cdot \mathbf{w}_k \right|^2 \right\} \right] \frac{\alpha P}{M}}{N_T E \left\{ \sin^2 \theta \right\} \sum_{\substack{m=1 \\ m \neq k}}^M E \left\{ \left| \mathbf{g}_k \cdot \mathbf{w}_m \right|^2 \right\} \frac{\alpha P}{M} + \sigma_n^2}. \tag{3-4}
\end{aligned}$$

Assume that the quantization region of a codeword has a perfect circular shape, corresponding to the quantization upper-bound [6]. Then, the quantization region of the  $i$ -th codeword  $\mathbf{c}_i$  can be defined by

$$R_i = \left\{ \mathbf{u} \mid \left| \mathbf{c}_i \cdot \mathbf{u} \right|^2 \geq \xi_{TH} \right\}. \tag{3-5}$$

where  $\xi_{TH}$  denotes a quantization threshold. Assuming that all the quantization regions  $\{R_1, R_2, \dots, R_{2^n}\}$  have the same area, the portion of each quantization region

with respect to the whole codebook surface can be represented as  $2^{-B}$ . Thus, the pdf of  $X_{\cos} = \cos^2 \theta$  can be represented as

$$f_{X_{\cos}}(x) = \begin{cases} \frac{(1-x)^{N_T-2}}{\int_{\xi_{TH}}^1 (1-u)^{N_T-2} du}, & \xi_{TH} \leq x \leq 1 \\ 0, & \text{otherwise} \end{cases} \quad (3-6)$$

where  $\xi_{TH}$  satisfies the following condition

$$\int_{\xi_{TH}}^1 f_{X_D}(x) dx = 2^{-B}. \quad (3-7)$$

Thus, the threshold  $\xi_{TH}$  can be determined as

$$\xi_{TH} = 1 - 2^{-\frac{B}{N_T-1}}. \quad (3-8)$$

Equation (3-6) can be rewritten as

$$f_{X_{\cos}}(x) = \begin{cases} 2^B (N_T - 1) (1-x)^{N_T-2}, & 1 - 2^{-\frac{B}{N_T-1}} \leq x \leq 1. \\ 0, & \text{otherwise} \end{cases} \quad (3-9)$$

The cumulative distribution function (cdf) of  $\cos^2 \theta$  can be represented as

$$F_{X_{\cos}}(x) = \begin{cases} 0, & x < 1 - 2^{-\frac{B}{N_T-1}} \\ 1 - 2^B (1-x)^{N_T-1}, & 1 - 2^{-\frac{B}{N_T-1}} \leq x \leq 1. \\ 1, & x > 1 \end{cases} \quad (3-10)$$

It can be shown that

$$\begin{aligned}
E\{X_{\cos}\} &= \int_{1-2^{-\frac{B}{N_T-1}}}^1 x f_{X_{\cos}}(x) dx \\
&= \int_0^1 F_{X_{\cos}}^{-1}(y) dy \\
&= \int_0^1 1 - (2^{-B}(1-y))^{\frac{1}{N_T-1}} dy \\
&= 1 - \frac{N_T-1}{N_T} 2^{-\frac{B}{N_T-1}}.
\end{aligned} \tag{3-11}$$

Since  $X_{\sin} = \sin^2 \theta = 1 - \cos^2 \theta$ , it can easily be shown that

$$E\{X_{\sin}\} = \frac{N_T-1}{N_T} 2^{-\frac{B}{N_T-1}}. \tag{3-12}$$

The beam weight vectors in (2-5) are  $N_T$ -dimensional vectors randomly distributed in  $(N_T - M + 1)$ -dimensional null-space of  $\mathbf{h}_m$ , where  $m \in \Psi$  and  $m \neq k$ . Thus, they have a degree of freedom (DoF) of  $N_T - M + 1$ . Since  $\mathbf{w}_k$  is determined to satisfy (2-4), it can be shown that

$$E\left\{\left|\hat{\mathbf{h}}_k \cdot \mathbf{w}_k\right|^2\right\} = \frac{N_T - M + 1}{N_T}. \tag{3-13}$$

Similarly,  $\mathbf{w}_m$  is a unit vector orthogonal to  $\hat{\mathbf{h}}_k$ , where  $m \in \Psi$  and  $m \neq k$ . It can be seen from (3-2) that  $\mathbf{g}_k \cdot \mathbf{w}_m$  is an inner product of two independent unit vectors randomly distributed in an  $N_T$ -dimensional space with a DoF of  $N_T - 1$ , which implies that  $\left|\mathbf{g}_k \cdot \mathbf{w}_m\right|^2$  has Beta distribution with  $\alpha = 1$  and  $\beta = N_T - 2$ . Thus, it can be shown that

$$E\{|\mathbf{g}_k \cdot \mathbf{w}_m|^2\} = \frac{1}{N_T - 1}. \quad (3-14)$$

As illustrated in Fig. 3.1, define  $\mathbf{g}_k^*$  by

$$\mathbf{g}_k^* = \frac{\mathbf{w}_k - (\mathbf{w}_k \cdot \hat{\mathbf{h}}_k) \hat{\mathbf{h}}_k}{\|\mathbf{w}_k - (\mathbf{w}_k \cdot \hat{\mathbf{h}}_k) \hat{\mathbf{h}}_k\|}. \quad (3-15)$$

Then, it can be shown that

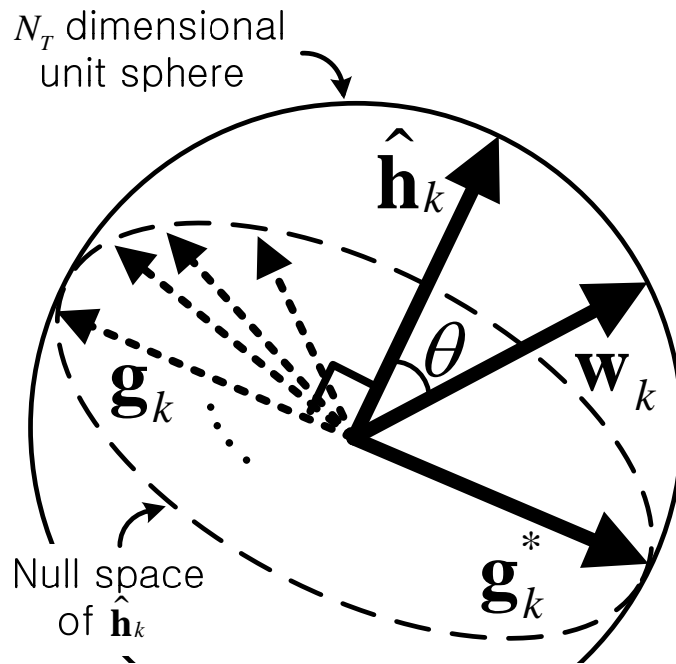


Fig. 3. 1. Visual representation of  $\hat{\mathbf{h}}_k$ ,  $\mathbf{w}_k$ ,  $\mathbf{g}_k^*$ , and  $\mathbf{g}_k$



$$\mathbf{w}_k = \cos \varphi \hat{\mathbf{h}}_k + \sin \varphi \mathbf{g}_k^* \quad (3-16)$$

where  $\varphi$  denotes the angle between  $\hat{\mathbf{h}}_k$  and  $\mathbf{w}_k$ . It can be shown from the above results that

$$\begin{aligned} E\left\{|\mathbf{g}_k \cdot \mathbf{w}_k|^2\right\} &= E\left\{\left|\mathbf{g}_k \cdot \left(\cos \varphi \hat{\mathbf{h}}_k + \sin \varphi \mathbf{g}_k^*\right)\right|^2\right\} \\ &= E\left\{|\sin \varphi|^2\right\} E\left\{|\mathbf{g}_k \cdot \mathbf{g}_k^*|^2\right\} \\ &= \left(1 - E\left\{|\hat{\mathbf{h}}_k \cdot \mathbf{w}_k|^2\right\}\right) E\left\{|\mathbf{g}_k \cdot \mathbf{g}_k^*|^2\right\}. \end{aligned} \quad (3-17)$$

Since  $\mathbf{g}_k$  has a DoF of  $(N_T - 1)$ ,  $|\mathbf{g}_k \cdot \mathbf{g}_k^*|^2$  has Beta distribution with  $\alpha = 1$  and  $\beta = N_T - 2$ . It can be represented as

$$E\left\{|\mathbf{g}_k \cdot \mathbf{w}_k|^2\right\} = \frac{M-1}{N_T(N_T-1)} \quad (3-18)$$

It can be shown from the above results that (3-4) can be rewritten as

$$\begin{aligned} \bar{\gamma}_k &\approx \frac{\frac{\alpha N_T P}{M} \left\{ \left(1 - \frac{N_T - 1}{N_T} 2^{-\frac{B}{N_T - 1}}\right) \left(\frac{N_T - M + 1}{N_T}\right) + \left(\frac{N_T - 1}{N_T} 2^{-\frac{B}{N_T - 1}}\right) \left(\frac{M - 1}{N_T(N_T - 1)}\right) \right\}}{\frac{\alpha N_T P}{M} \left(\frac{N_T - 1}{N_T} 2^{-\frac{B}{N_T - 1}}\right) \sum_{\substack{m=1 \\ m \neq k}}^M \left(\frac{1}{N_T - 1}\right) + \sigma_n^2} \\ &= \frac{\frac{\alpha P}{M} \left\{ (N_T - M + 1) + (M - N_T) 2^{-\frac{B}{N_T - 1}} \right\}}{\frac{\alpha P}{M} (M - 1) 2^{-\frac{B}{N_T - 1}} + \sigma_n^2}. \end{aligned} \quad (3-19)$$

When the quantization bit size  $B$  is sufficiently large, (3-19) can be

approximated as

$$\bar{\gamma}_k \approx \frac{\alpha P}{M \sigma_n^2} (N_T - M + 1). \quad (3-20)$$

Then, the mean of the ergodic spectral efficiency can be represented as

$$\begin{aligned} E\{C_{tot}\} &= E\{M \log_2(1 + \gamma_k)\} \\ &\approx M \log_2(1 + E\{\gamma_k\}) \\ &\approx M \log_2\left\{1 + \frac{\alpha P}{M \sigma_n^2} (N_T - M + 1)\right\}. \end{aligned} \quad (3-21)$$

It can be seen that it increases as  $M$  increases, as shown in Fig. 3.2. (a). It is desirable to use spatial multiplexing with a full order of  $N_T$ , when the CDI is ideal.

However, CDI quantization bit size can be approximated as the number of transmit antennas in practical environments [12]. For  $M \geq 2$ , it can be shown that

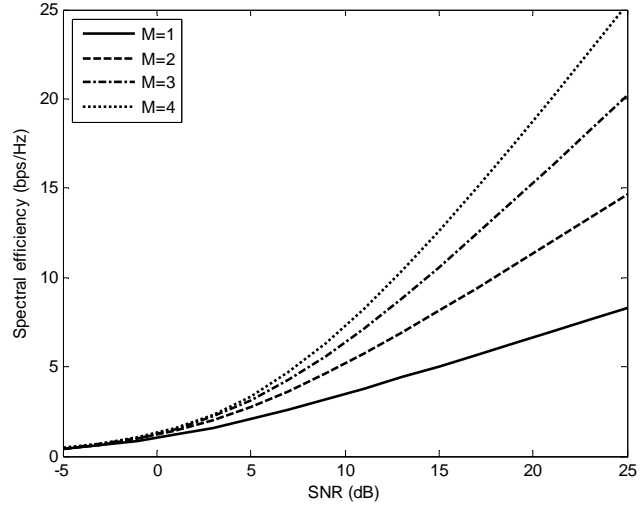
$$E\{C_{tot}\} \leq M \log_2\left(1 + \frac{N_T - M + 1}{M - 1} 2^{\frac{B}{N_T - 1}} + \frac{M - N_T}{M - 1}\right) \quad (3-22)$$

where the equality holds when  $P/\sigma_n^2 \rightarrow \infty$ . When  $M = 1$ , it can be shown that

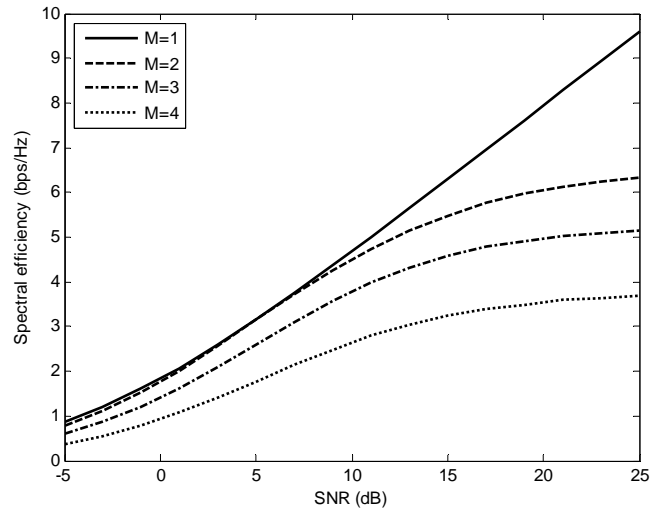
$$E\{C_{tot}\} \approx \log_2\left\{1 + \frac{\alpha P}{M \sigma_n^2} \left(N_T + (1 - N_T) 2^{\frac{B}{N_T - 1}}\right)\right\}. \quad (3-23)$$

The ergodic spectral efficiency linearly increases as the average SNR  $P/\sigma_n^2$  increases. It can be seen from (3-22) and (3-23) that when the average SNR is sufficiently large, the ergodic spectral efficiency of the MUSM is limited by the inter-

beam interference mainly due to the CDI quantization error, yielding performance inferior to the SUBF. Fig. 3.2. (b) depicts the spectral efficiency with the use of a codebook of four-bit size. It can be seen from Fig. 3.2. (b) that unless the use of a codebook with a large bit size, it is not desirable to use MUSM, as shown in the analysis.



(a) Ideal case (no quantization error, or  $B = \infty$ )



(b) The use of a four-bit codebook

**Fig. 3. 2. Spectral efficiency of zero-forcing beamforming ( $N_r = 4$ )**

## 3.2. Previous opportunistic CSI feedback schemes

A number of opportunistic CSI feedback schemes have been proposed for the improvement of spectral efficiency [7]-[9]. In this section, we briefly review previous opportunistic CSI feedback schemes.

### 3.2.1. Absolute SNR-based single user scheduling (ASS)

The ASS scheme allows user  $k$  to report its CSI to the BS only if [7]

$$k \in \Theta_{ASS} \triangleq \{i \mid \zeta_i > \zeta_{TH}\} \quad (3-24)$$

where  $\zeta_i (= \alpha P \|\mathbf{h}_i\|^2 / \sigma_n^2)$  denotes the instantaneous SNR of user  $i$  and  $\zeta_{TH}$  is a threshold to be determined by the BS. The BS selects a user with the largest SNR as

$$i^* = \arg \max_{i \in \Theta_{ASS}} (\zeta_i). \quad (3-25)$$

The ASS scheme can reduce the signaling overhead for the CSI feedback by exploiting selective MUD. However, it may suffer from scheduling fairness since users in good channel condition can be serviced.

### 3.2.2. Normalized SNR-based scheduling (NSS)

The NSS scheme was proposed to alleviate the scheduling fairness problem in the ASS scheme [7]. It allows user  $k$  to report its CSI to the BS only when the CQI normalized with respect to the average SNR exceeds a threshold as

$$k \in \Theta_{NSS} \triangleq \left\{ i \mid \eta_i = \frac{\zeta_i}{E\{\zeta_i\}} > \eta_{TH} \right\} \quad (3-26)$$

where  $\eta_{TH}$  is a threshold to be determined by the BS and  $\eta_i$  denotes the normalized SNR of user  $i$ . The BS selects a user as

$$i^* = \arg \max_{i \in \Theta_{NSS}} (\eta_i). \quad (3-27)$$

Thus, the NSS can improve the user scheduling fairness while exploiting the MUD gain.

### 3.2.3. Advanced normalized SNR-based scheduling (A-NSS)

The spatial correlation may affect the variance of user SNR in MIMO environments. When users experience the same average SNR with different variance, users with higher fluctuation of SNR (i.e., larger variance of the SNR) may have more chances to be serviced in opportunistic user scheduling environments. The A-NSS scheme considers the normalization of SNR in terms of the mean and variance of SNR as

$$k \in \Theta_{A-NSS} \triangleq \left\{ i \mid \xi_i = \frac{\zeta_i - E\{\zeta_i\}}{\sqrt{\text{Var}\{\zeta_i\}}} > \xi_{TH} \right\}. \quad (3-28)$$

where  $\xi_i$  denotes the normalized SNR of user  $i$ ,  $\xi_{TH}$  is a threshold and  $\text{Var}\{X\}$  denotes the variance of  $X$ .

The BS selects a user as

$$i^* = \arg \max_{i \in \Theta_{A-NSS}} (\xi_i). \quad (3-29)$$

Thus, the A-NSS can improve the user scheduling fairness compared to the NSS scheme.

### 3.2.4. Limitation in the opportunistic CSI feedback schemes

The previous opportunistic CSI feedback schemes mainly consider the CQI for the CSI feedback and user scheduling. They quite effectively work when applied to the SUBF schemes with the use of perfect CDI. However, they may experience the reduction of beamforming gain in the presence of CDI quantization error. When applied to the MUSM schemes, they may suffer from severe performance degradation mainly due to the inter-beam interference. It is desirable to consider the effect of CDI quantization error on the opportunistic CSI feedback.

## 4. Proposed opportunistic CSI feedback

In this section, we propose a novel opportunistic CSI feedback scheme. We consider the use of CBF and ZFBF for the SUBF and the MUSM, respectively.

### 4.1. Single-user beamforming

When the BS serves a single user with CBF (i.e.,  $M = 1$ ), (3-1) can be rewritten as

$$\begin{aligned}\gamma_k &= |\mathbf{h}_k \cdot \mathbf{w}_k|^2 \frac{\alpha P}{\sigma_n^2} \\ &= \mu_k \frac{\alpha P}{\sigma_n^2}.\end{aligned}\tag{4-1}$$

With the use of instantaneous SNR normalized with respect to its average, the channel gain  $\mu_k$  can be used as a metric for the proposed opportunistic CSI feedback. User  $k$  can report its channel information to the BS only when

$$k \in \Theta_{SUBF} \triangleq \{i \mid \mu_k > \mu_{TH}\}\tag{4-2}$$

where  $\mu_{TH}$  is a threshold to be determined. Among users who reported their CSI, the BS can select a user as



$$i^* = \arg \max_{i \in \Theta_{SUBF}} (\mu_i). \quad (4-3)$$

Since

$$\begin{aligned} \mu_i &= \|\mathbf{h}_i\|^2 \cos^2 \theta \\ &= X_p X_{\cos}, \end{aligned} \quad (4-4)$$

the pdf of  $\mu_i$  can be represented as [13]

$$f_\mu(x) = \int_{-\infty}^{\infty} \frac{1}{|y|} f_{X_p}(y) f_{X_{\cos}}\left(\frac{x}{y}\right) dy. \quad (4-5)$$

Here, the pdf of  $X_p$  and  $X_{\cos}$  is represented as (2-9) and (3-9), respectively. (4-5)

can further be simplified to

$$\begin{aligned} f_\mu(x) &= \frac{2^B}{\Gamma(N_T - 1)} \times \int_x^{1-x} e^{-y} (y-x)^{N_T-2} dy \\ &= 2^B \times \left[ e^{-x} - e^{-\frac{1}{1-s}x} \sum_{n=0}^{N_T-2} \left\{ \frac{1}{\Gamma(n+1)} \left( \frac{s}{1-s} x \right)^n \right\} \right] \\ &= 2^B e^{-\frac{1}{1-s}x} \sum_{n=N_T-1}^{\infty} \left\{ \frac{1}{\Gamma(n+1)} \left( \frac{s}{1-s} x \right)^n \right\}, \text{ for } x \geq 0 \end{aligned} \quad (4-6)$$

where  $s = 2^{-\frac{B}{N_T-1}}$ . The cdf of  $\mu_i$  can be represented as

$$\begin{aligned} F_\mu(x) &= \int_0^x f_\mu(t) dt \\ &= 2^B \sum_{n=N_T-1}^{\infty} \left\{ \frac{s^n}{\Gamma(n+1)} \int_0^x \left( \frac{1}{1-s} t \right)^n e^{-\frac{1}{1-s}t} dt \right\} \\ &= 2^B \sum_{n=N_T-1}^{\infty} \left[ \frac{s^n}{\Gamma(n+1)} \{1 - \Gamma(n+1, (1-s)x)\} \right] \end{aligned} \quad (4-7)$$

where  $\Gamma(\cdot, \cdot)$  denotes the incomplete Gamma function.

Define the outage of the CSI feedback scheme by

$$\text{card}(\Theta_{SUBF}) = 0 \quad (4-8)$$

where  $\text{card}(A)$  denotes the cardinality of a set  $A$ . Assuming that  $\mu_1, \mu_2, \dots, \mu_K$  are i.i.d., the probability that  $n$  users report the CSI can be represented as

$$P_N(n) = \binom{K}{n} (F_\mu(\mu_{TH}))^{K-n} (1 - F_\mu(\mu_{TH}))^n. \quad (4-9)$$

It can be shown that the average number of CSI reporting users is represented as

$$E\{N\} = K \times F_\mu(\mu_{TH}). \quad (4-10)$$

The corresponding outage probability of the proposed scheme can be represented as

$$P_{out} = (F_\mu(\mu_{TH}))^K. \quad (4-11)$$

The BS can determine the threshold  $\mu_{TH}$  according to the target outage probability as

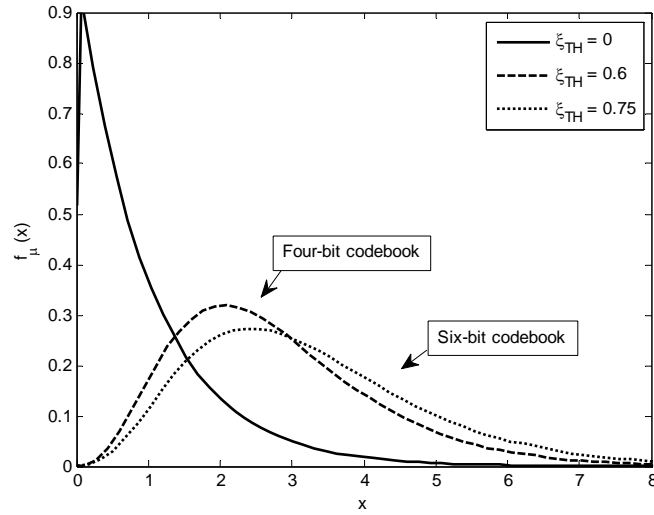
$$\mu_{TH} = F_\mu^{-1} \left( (P_{out}^{(Target)})^{\frac{1}{K}} \right) \quad (4-12)$$

where  $P_{out}^{(Target)}$  denotes the target outage probability. Or, it can determine the threshold  $\varepsilon_{TH}$  for a target average number of CSI reporting users as

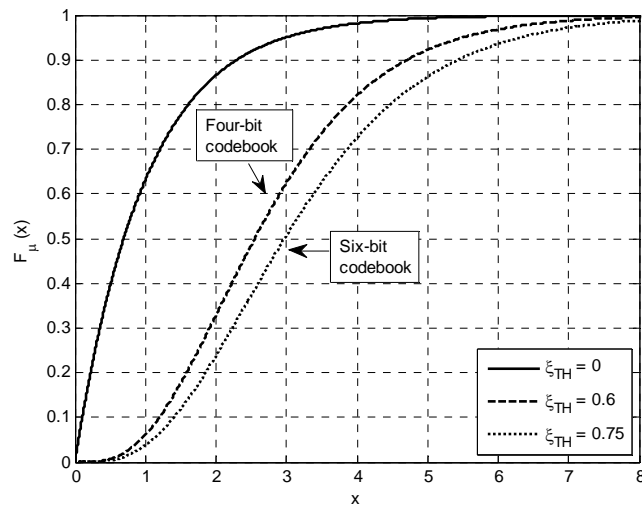
$$\mu_{TH} = F_{\mu}^{-1} \left( \frac{N_{average}^{(Target)}}{K} \right) \quad (4-13)$$

where  $N_{average}^{(Target)}$  denotes the target average number of CSI reporting users.

Fig. 4 depicts the pdf and cdf of  $\mu$  for various values of  $\xi_{TH}$  when  $N_T = 4$ . The threshold  $\mu_{TH}$  can be determined in consideration of the desired number of users reporting the CSI and/or the required outage probability.



(a) The pdf of  $\mu$



(b) The cdf of  $\mu$

**Fig. 4. 1.** The pdf and cdf of  $\mu$  when  $N_T = 4$ .

## 4.2. Multi-user spatial multiplexing

It is desirable to generate multiple beams for users in good channel condition. The proposed scheme considers the maximum of the post SNR in (3-1) for the spatial multiplexing, i.e.,

$$\max(\gamma_k) = \max \left( \frac{\|\mathbf{h}_k\|^2 |\tilde{\mathbf{h}}_k \cdot \mathbf{w}_k|^2 \frac{\alpha P}{M}}{\|\mathbf{h}_k\|^2 \sum_{\substack{m=1 \\ m \neq k}}^M |\tilde{\mathbf{h}}_k \cdot \mathbf{w}_m|^2 \frac{\alpha P}{M} + \sigma_n^2} \right). \quad (4-14)$$

When the average SNR is sufficiently high, it can be approximated as

$$\begin{aligned} \max(\gamma_k) &\approx \max \left( \frac{\|\mathbf{h}_k\|^2 |\tilde{\mathbf{h}}_k \cdot \mathbf{w}_k|^2 \frac{\alpha P}{M}}{\|\mathbf{h}_k\|^2 \sum_{\substack{m=1 \\ m \neq k}}^M |\tilde{\mathbf{h}}_k \cdot \mathbf{w}_m|^2 \frac{\alpha P}{M}} \right) \\ &= \max \left( \frac{|\tilde{\mathbf{h}}_k \cdot \mathbf{w}_k|^2}{\sum_{\substack{m=1 \\ m \neq k}}^M |\tilde{\mathbf{h}}_k \cdot \mathbf{w}_m|^2} \right) \\ &= \max \left( \frac{\cos^2 \theta |\hat{\mathbf{h}}_k \cdot \mathbf{w}_k|^2 + \sin^2 \theta |\mathbf{g}_k \cdot \mathbf{w}_k|^2 + 2 \cos \theta \sin \theta \{(\hat{\mathbf{h}}_k \cdot \mathbf{w}_k)(\mathbf{g}_k \cdot \mathbf{w}_k)\}}{\sin^2 \theta \sum_{\substack{m=1 \\ m \neq k}}^M |\mathbf{g}_k \cdot \mathbf{w}_m|^2} \right). \end{aligned} \quad (4-15)$$

It can be seen that the minimization of  $\theta$  and the magnitude of  $\mathbf{g}_k$  can maximize  $\gamma_k$ . This implies that the CDI quantization error should be minimized. Thus, it may be desirable to make user  $k$  report its CSI when

$$k \in \Theta_{MUSM} \triangleq \left\{ i \mid \varepsilon_i = 1 - \left| \hat{\mathbf{h}}_i \cdot \tilde{\mathbf{h}}_i \right|^2 < \varepsilon_{TH} \right\} \quad (4-16)$$

where  $\varepsilon_i$  denotes the CDI quantization error of user  $i$  and  $\varepsilon_{TH}$  is a threshold.

The probability that the instantaneous CSI satisfies the condition (4-16) can be represented as

$$\begin{aligned} p_F &= \frac{\int_{1-\varepsilon_{TH}}^1 f_{X_D}(x) dx}{\int_{1-2^{-\frac{B}{N_T-1}}}^1 f_{X_D}(x) dx} \\ &= 2^B \varepsilon_{TH}^{N_T-1}. \end{aligned} \quad (4-17)$$

The corresponding probability mass function of the number of CSI reporting users can be represented as

$$\begin{aligned} p_N(n) &= \binom{K}{n} (1-p_F)^{K-n} p_F^n \\ &= \binom{K}{n} (1-2^B \varepsilon_{TH}^{N_T-1})^{K-n} (2^B \varepsilon_{TH}^{N_T-1})^n. \end{aligned} \quad (4-18)$$

It can be shown that the average number of CSI reporting users can be represented as

$$E\{N\} = 2^B \varepsilon_{TH}^{N_T-1} K. \quad (4-19)$$

The corresponding outage probability is defined by the probability mass function of the number of CSI reporting users when the number of CSI reporting users is zero, i.e.,

$$\begin{aligned}
P_{out} &= P_N(0) \\
&= \left(1 - 2^B \varepsilon_{TH}^{N_T-1}\right)^K.
\end{aligned} \tag{4-20}$$

The BS can determine the threshold  $\varepsilon_{TH}$  according to the target outage probability as

$$\varepsilon_{TH} = 2^{-\frac{B}{N_T-1}} \left\{ 1 - \left( P_{out}^{(Target)} \right)^{\frac{1}{K}} \right\}^{\frac{1}{N_T-1}} \tag{4-21}$$

where  $P_{out}^{(Target)}$  denotes the target outage probability. Or, it can determine the threshold  $\varepsilon_{TH}$  for a target average number of CSI reporting users as

$$\varepsilon_{TH} = \left( \frac{N_{average}^{(Target)}}{2^B K} \right)^{\frac{1}{N_T-1}} \tag{4-22}$$

where  $N_{average}^{(Target)}$  denotes the target average number of CSI reporting users.

It can be shown that the proposed scheme can provide the expected capacity with the use of random user scheduling, approximately represented as

$$E\{C_{tot}\} \simeq \begin{cases} M \log_2 \left( 1 + \frac{\frac{\alpha P}{M} \left( (N_T - M + 1) + (M - N_T) \varepsilon_{TH} \right)}{\frac{\alpha P}{M} (M - 1) \varepsilon_{TH} + \sigma_n^2} \right), & n > M \\ n \log_2 \left( 1 + \frac{\frac{\alpha P}{n} \left( (N_T - n + 1) + (n - N_T) \varepsilon_{TH} \right)}{\frac{\alpha P}{n} (n - 1) \varepsilon_{TH} + \sigma_n^2} \right), & 1 \leq n \leq M \end{cases}. \tag{4-23}$$

It can be seen that the random scheduling does not provide an additional MUD gain

when the number of CSI reporting users is larger than the target multiplexing order (i.e.,  $n \geq M$ ). This problem can be alleviated by selecting users based on the CDI as

$$\Omega^* = \arg \min_{\Omega} \left( \sum_{i \in \Omega} \sum_{\substack{j \in \Omega \\ j \neq i}} |\hat{\mathbf{h}}_i \cdot \hat{\mathbf{h}}_j|^2 \right). \quad (4-24)$$

where  $\Omega^*$  denotes the set of users selected by the user scheduler.

### 4.3. Performance evaluation

The performance of the proposed opportunistic CSI feedback scheme is evaluated by computer simulation. It is assumed that the BS utilizes four transmit antennas for the signal transmission and the user CDI is encoded using a four-bit codebook. The main simulation parameters are summarized in Table 4.1.

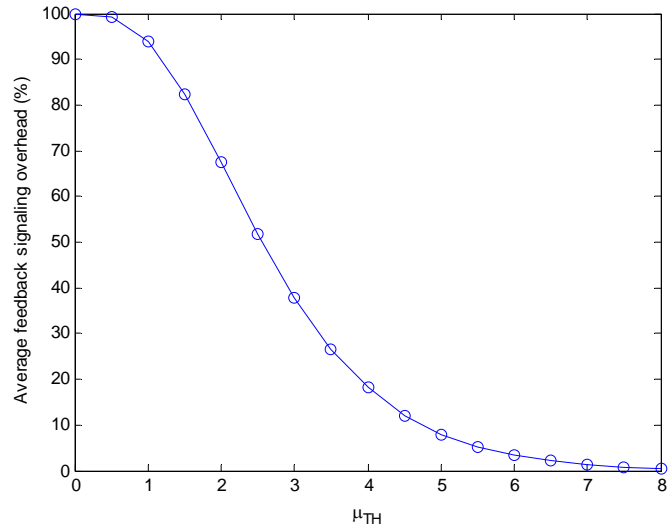
Fig. 4.2 depicts the performance of the proposed scheme in single user beamforming environments, where the average SNR is set to 0dB. It can be seen from Fig. 4.2 (a) and (b) that as the threshold increases, the amount of CSI feedback signaling overhead decreases, but the outage probability increases. It can be seen from Fig. 4.2 (c) that the proposed scheme can provide high spectral efficiency while significantly reducing the amount of CSI feedback signaling overhead by adjusting the threshold. It can be seen from Fig. 4.2 (d) and (e) that the proposed scheme can provide better performance than the NSS by additionally taking into consideration of CDI, while



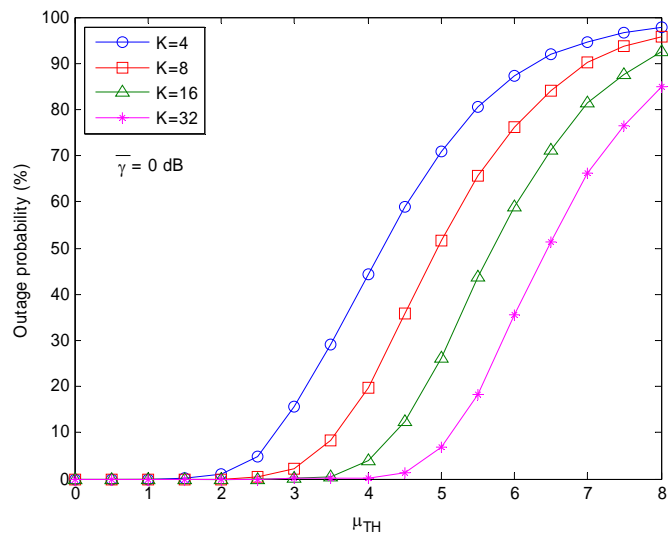
using a similar amount of CSI feedback signaling overhead.

**Table. 4. 1. Simulation parameter**

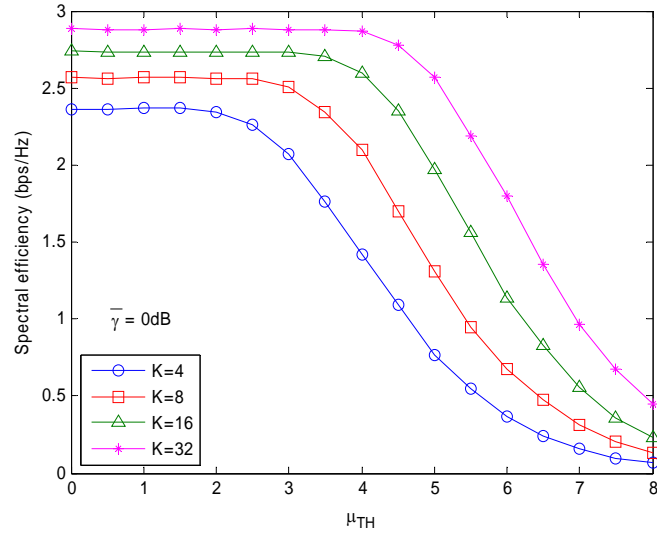
Simulation parameters	Values
Antenna configuration	BS: 4, user: 1
Average SNR	SUBF: 0 dB, MUSM: 15 dB
CDI quantization bits	4 bits [12]
Number of users	4 / 8 / 16 / 32
Spatial multiplexing scheme	Zero-forcing beamforming
Multiplexing order	2
Channel model	Rayleigh (Jake's spectrum)
Spatial channel distribution	i.i.d.



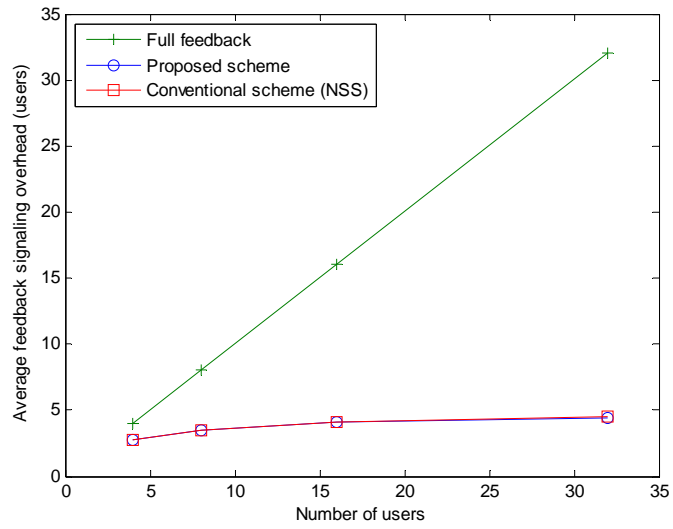
(a) Average feedback signaling overhead



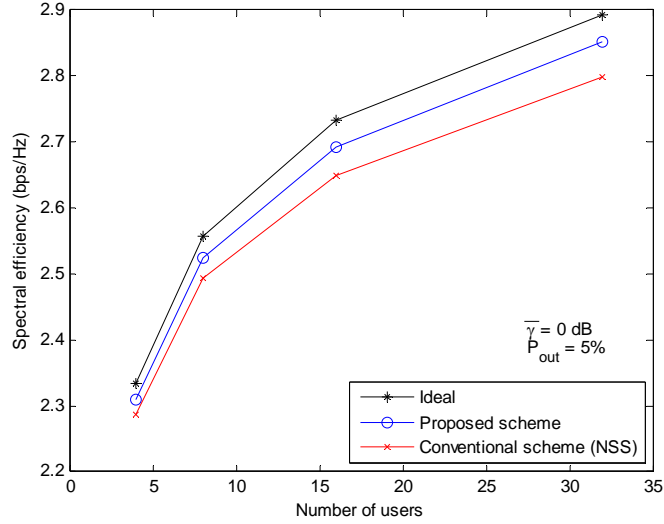
(b) Outage probability



(c) Spectral efficiency



(d) Comparison of feedback signaling overhead

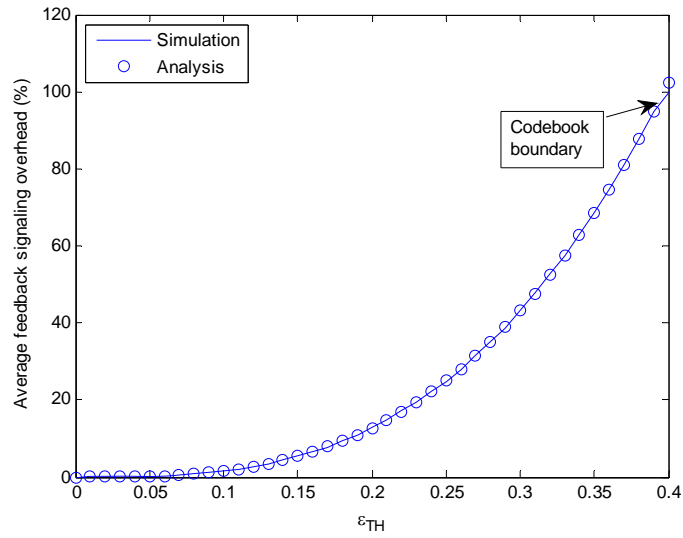


(e) Comparison of spectral efficiency

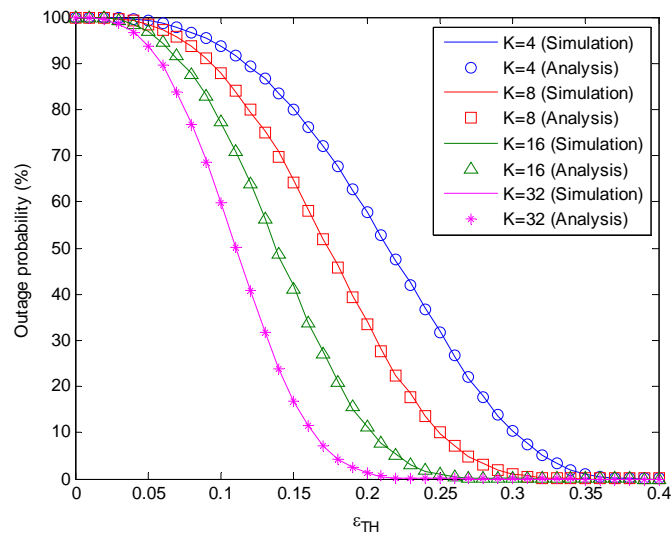
**Fig. 4. 2. Performance of the proposed scheme with single-user beamforming.**

Fig. 4.3 depicts the performance of the proposed scheme in MUSM environments, where the average SNR is set to 15dB. It can be seen from Fig. 4.3 (a) and (b) that as the threshold  $\epsilon_{TH}$  increases, the outage probability decreases, while the feedback signaling overhead increases. It can be seen from Fig. 4.3 (c) that as the threshold  $\epsilon_{TH}$  increases, the inter-beam interference increases mainly due to the quantization error. It can be seen from Fig. 4.3 (d) that the spectral efficiency can be maximized when the threshold is determined to yield low outage probability and low inter-beam interference as well. It can be seen from Fig. 4.3 (e) and (f) that the proposed scheme outperforms the CQI based opportunistic feedback scheme, while using a similar

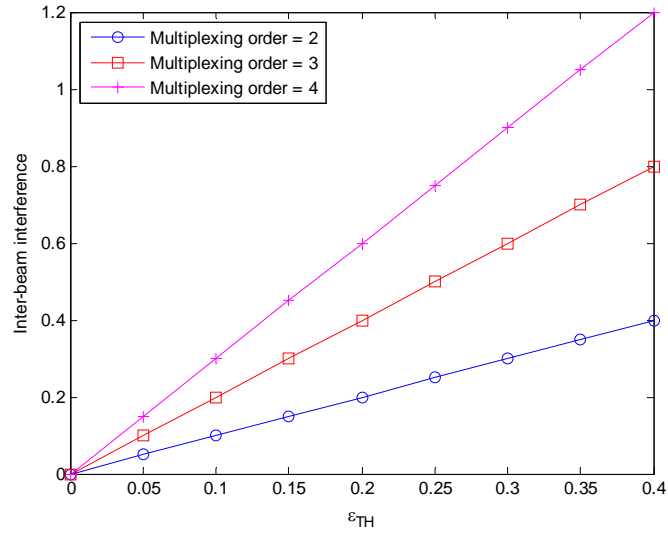
amount of CSI feedback signaling overhead.



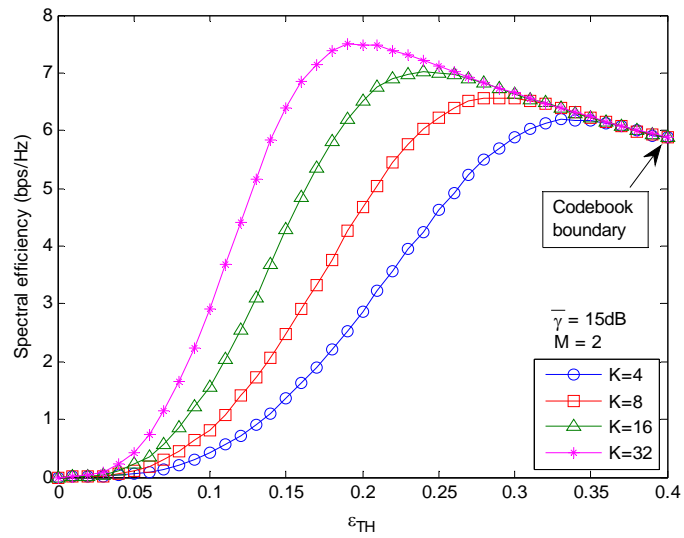
(a) Average feedback signaling overhead



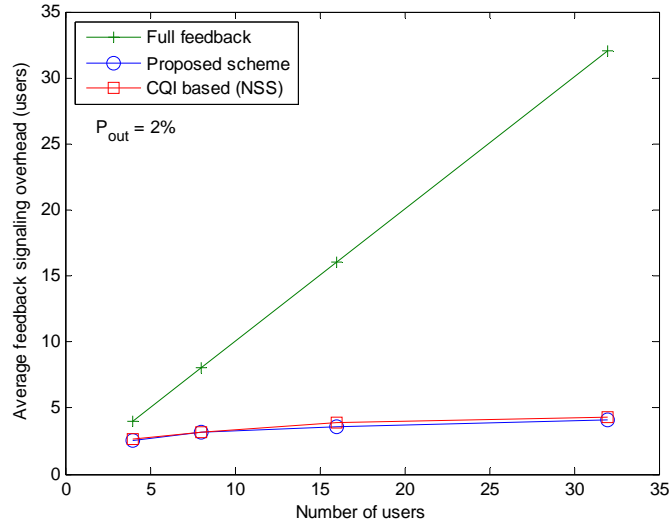
(b) Outage probability



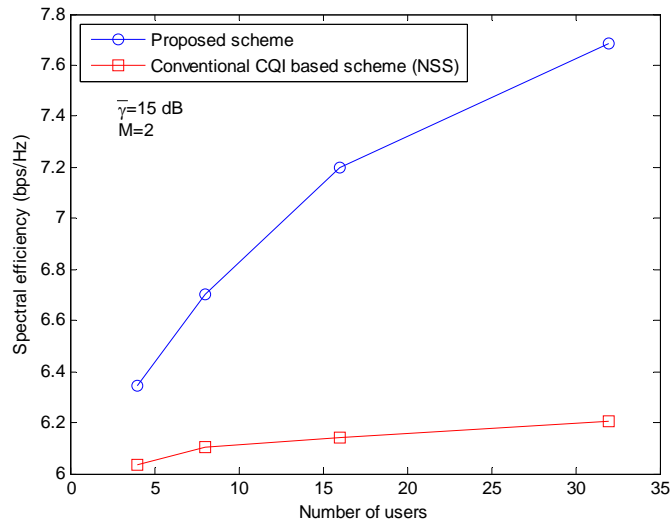
(c) Inter-beam interference



(d) Spectral efficiency



(e) Comparison of feedback signaling overhead



(f) Comparison of spectral efficiency

**Fig. 4. 3. Performance of the proposed scheme with multi-user spatial multiplexing.**



## 5. Conclusions

In this thesis, we have considered opportunistic CSI feedback in multi-user MIMO environments. We have shown that the MIMO performance may seriously be affected by the CDI quantization error. To alleviate this problem, the proposed opportunistic CSI feedback scheme allows users to report their CSI by considering the CDI quantization error as well as the CQI in single- and multi-user MIMO environments. It can almost fully achieve the multi-user diversity gain without increasing the feedback signaling overhead, noticeably outperforming the NSS scheme which only considers the CQI. It can also alleviate the inter-beam interference problem by allowing users to report their CSI only when the CDI quantization error is small. Finally, the performance of the proposed scheme has been verified by computer simulation, showing the effectiveness of the proposed scheme.

It is of great concern to improve the system spectral efficiency for higher throughput, which can be achieved by means of cooperative transmission among multiple BSs with the use of massive MIMO schemes. Thus, the reduction of signaling overhead for the CSI feedback is one of major issues to be further studied for the implementation in multi-cell cooperation environments.

## References

- [1] G. Caire and S. Shamai, “On the achievable throughput of a multi-antenna Gaussian broadcast channel,” *IEEE Trans. Inf. Theory*, vol. 49, no. 7, pp. 1691–1706, July 2003.
- [2] A. Goldsmith, S. A. Jafar, and S. Vishwanath, “Capacity limits of MIMO channels,” *IEEE J. Sel. Areas Commun.*, vol. 21, no. 5, pp. 684–702, June 2003.
- [3] L. Liu, R. Chen, S. Geirhofer, K. Sayana, Z. Shi, and Y. Zhou, “Downlink MIMO in LTE-advanced: SU-MIMO vs. MU-MIMO,” *IEEE Comms. magazine*, vol. 50, no. 2, pp. 140–147, Feb. 2012.
- [4] A. Goldsmith, “Wireless communications,” Cambridge University Press, 2005.
- [5] K. -W. Lee, H. -N. Cho, and Y. -H. Lee, “Performance of general order selection diversity in spatially correlated Rayleigh fading channel,” in *Proc. ITA workshop*, Feb. 2011.
- [6] T. Yoo, N. Jindal and A. Goldsmith, “Multi-antenna downlink channels with limited feedback and user selection,” *IEEE J. Sel. Areas Commun.*, vol.25, no.7, pp.1478–1491, July 2007.

- [7] D. Gesbert and M. -S. Alouini, "How much feedback is Multi-User Diversity really worth?," in *Proc. IEEE ICC'04*, p. 234, June 2004.
- [8] L. Yang and M. -S. Alouini, "Performance analysis of multiuser selection diversity," *IEEE Trans. Veh. Technol.*, vol. 55, no. 6, pp. 1848–1861, Nov. 2006.
- [9] G. -S. Heo, J. -S. Park, Y. -S. Byun, and Y. -H. Lee, "Opportunistic user scheduling with normalized CQI in heterogeneous channel environments," in *Proc. WoWMoM'12*, pp. 1–3, June 2012.
- [9] K. Kusume, G. Dietl, T. Abe, H. Taoka, S. Nagata, "System level performance of downlink MU-MIMO transmission for 3GPP LTE-Advanced," in *Proc. IEEE VTC'10*, pp. 1–5, May 2010.
- [10] C. Zhang, W. Xu, M. Chen, "Hybrid zero-forcing beamforming/orthogonal beamforming with user selection for MIMO broadcast channels," *IEEE Communications Letters*, vol. 13, no. 1, pp. 10-12, Jan. 2009.
- [11] D. Tse and P. Viswanath, "Fundamentals of wireless communication," Cambridge University Press, 2005.
- [12] 3GPP TS36.211 v10.4.0 "Evolved Universal Terrestrial Radio Access (E-UTRA); Physical Channels and Modulation (Release 10)," Dec. 2011.
- [13] V. K. Rohatgi "An introduction to probability theory mathematical statistics," Wiley, New York, 1976.

## 초 록

최근 다중 입력 다중 출력(MIMO) 기법은 무선 통신 환경에서 데이터 전송률을 향상시키기 위한 방안으로 각광받고 있다. 기지국은 다중 송신 안테나를 이용하여 단일 사용자의 신호 대 간섭비(SNR)를 향상시킬 수 있다. 또한 기지국이 다중 송신 안테나를 이용하여 다중 빔을 생성하고, 같은 시간-주파수 자원에서 동시에 여러 명의 사용자를 서비스 할 수 있다. MIMO 시스템 운용을 위해서는 채널 품질 정보(CQI)와 채널 방향 정보(CDI)로 이루어진 채널 상태 정보(CSI)가 필요하다. 채널 상태 정보는 사용자가 제한된 비트 수로 양자화 하여 기지국에게 전달한다. 이 때, 채널 정보의 양자화 오차는 심각한 수준의 성능 저하를 초래할 수 있다.

채널 상태 정보는 사용자들로부터 기회적으로 전달될 수 있으며, 이를 통해 피드백 오버헤드를 감소시키는 동시에 다중 사용자 다이버시티(MUD) 이득을 얻을 수 있다. 대부분의 기회적 채널 정보 피드백 기법들은 채널 품질 정보를 기준으로 피드백 여부를 결정한다. 그러나, 양자화된 채널 방향 정보를 사용하는 경우에는 빔 간의 간섭이 유발될 수 있다. 따라서, 채널 품질 정보뿐만 아니라 채널 방향 정보까지 함께 고려하는 것이 바람직하다.

본 논문에서는 채널 품질 정보와 채널 방향 정보를 함께 고려한 채널 상태 정보 피드백 기법을 고려한다. 먼저 채널 상태 정보의 양자화 오차가 단일 사용자 및 다중 사용자 MIMO 환경의 성능에 미치는 영향을 분석하고, 각 환경에 맞는 기회적 채널 정보 피드백 기술 및 사용자 스케줄링 기술을 제안한다. 제안 기법을 사용한 경우 채널 정보 피드백 오버헤드를 감소시키면서도 주파수 효율을 향상시킬 수 있음을 시뮬레이션 결과를 통해 알 수 있다.

**主要語:** 기회적 피드백, 코드북, 채널 방향정보, 빔포밍, 양자화 오차

**학번 :** 2010-23266